

Atomic ordering in $\text{Ca}_{x/2}\text{Al}_x\text{Si}_{1-x}\text{O}_2$ glasses ($x=0,0.34,0.5,0.68$) by energy-dispersive x-ray diffraction

V. Petkov

Department of Solid State Physics, Sofia University, Sofia 1126, Bulgaria

Th. Gerber and B. Himmel

Fachbereich Physik, Universität Rostock, Rostock D-18051, Germany

(Received 2 March 1998)

Extended structure factors for $\text{Ca}_{x/2}\text{Al}_x\text{Si}_{1-x}\text{O}_2$ glasses ($x=0,0.34,0.5,0.68$) have been obtained by energy-dispersive x-ray diffraction. The first neighbor Si-O and Al-O interatomic distances and coordination numbers have been determined thanks to the improved resolution of the experimental atomic distribution functions. It has been found that Al atoms are always fourfold coordinated by oxygen atoms while the oxygen coordination of Si atoms varies with the change of Al and Ca contents in the glasses investigated. The experimental information obtained has made it possible to discriminate between contradicting structure models for $\text{Ca}_{x/2}\text{Al}_x\text{Si}_{1-x}\text{O}_2$ glasses ($x=0,0.34,0.5,0.68$) that have been previously proposed. [S0163-1829(98)03842-9]

I. INTRODUCTION

Glasses of the system $\text{CaO-Al}_2\text{O}_3\text{-SiO}_2$ have been a subject of numerous studies in the last two decades. Several physical properties and thermodynamical characteristics have been systematically measured and the presence of relationship(s) between some properties of useful technological applications and composition has been looked for.¹⁻⁵ Since any such relationship(s) found empirically can only be explained on the basis of a structure model for the respective glasses a number of structural studies on calcium aluminate-silica glasses has been carried out. The most structural information has been acquired from spectroscopic methods such as ²⁹Si and ²⁷Al magic angle spinning (MAS)-NMR,⁶⁻⁸ Raman,^{9,10} x-ray photoemission spectroscopy,¹¹ electron spin resonance,¹² and IR.¹³ Wide-angle x-ray diffraction investigations have been carried out as well.¹⁴⁻¹⁶ Outcomes of these studies have suggested that at atomic scale $\text{CaO-Al}_2\text{O}_3\text{-SiO}_2$ glasses can be considered as a more or less polymerized network of Si-O and Al-O structural units with Ca cations occupying large, irregular sites within the network cavities.^{1,6,7,9,15,16} Depending on the chemical composition only the details in the just described model picture including the type of Al-O structural units (octahedral or tetrahedral), the connectivity of Si and Al polyhedra, and the presence and location of nonbridging oxygen atoms, have been found to vary. Unfortunately, structural models for given families of $\text{CaO-Al}_2\text{O}_3\text{-SiO}_2$ glasses that contradict in these important details have been put forward. In particular, two competing structure models have been suggested for glasses along the join silica (SiO_2) calcium aluminate (CaAl_2O_4). According to one of these models¹ all glasses along the join $\text{SiO}_2\text{-CaAl}_2\text{O}_4$ may be viewed as a fully polymerized network of interconnected SiO_4 and AlO_4 tetrahedral units where no nonbridging oxygens are present. According to the other model,^{6,12} glasses with compositions varying from that of pure silica (SiO_2) to that of anorthite ($\text{Ca}_{0.25}\text{Al}_{0.5}\text{Si}_{0.5}\text{O}_2$) have a fully polymerized network of SiO_4 and AlO_4 tetrahe-

dra. When, however, $(\text{CaO}+\text{Al}_2\text{O}_3)$ exceeds the SiO_2 content nonbridging oxygen atoms emerge. Therefore, glasses with composition varying from that of anorthite to that of calcium aluminate are formed of both regular and defect SiO_4 and AlO_4 units, i.e., these glasses do not have a fully polymerized tetrahedral network. To resolve this ambiguity a careful determination of the structure of $\text{Ca}_{x/2}\text{Al}_x\text{Si}_{1-x}\text{O}_2$ glasses ($x=0,0.34, 0.5,0.68$) and an identification of the type of SiO_4 and AlO_4 units obviously need to be carried out.

The structure of glassy materials is commonly described in terms of atomic distribution functions which reflect all interatomic correlations in the glassy material. These functions are most frequently obtained by diffraction methods employing x rays or neutrons. With the wide-angle diffraction method the x-ray photons (neutrons) scattered from the sample are recorded as a function of the angle 2Θ between the directions of the incoming and diffracted monochromatic radiation beams. On the basis of the diffraction spectrum recorded the so-called structure factor $S(q)$, which actually contains the experimentally accessible information about the atomic-scale structure of the glassy material, is obtained. From $S(q)$ the so-called reduced atomic distribution function $G(r) = 4\pi r[\rho(r) - \rho_0]$, is calculated as follows:

$$G(r) = (2/\pi) \int_{q=0}^{q=q_{\max}} q[S(q) - 1] \sin(qr) dq, \quad (1)$$

where r is the real space distance, $\rho(r)$ and ρ_0 are the local and average atomic number densities of the glassy material, respectively, and q is the wave (scattering) vector defined by the relation $q = (4\pi/\lambda) \sin(\Theta) = (4\pi/hc) E \sin(\Theta)$. Here λ and E are the wavelength and energy of the radiation used, h is Planck's constant, and c is the velocity of light. An inherent limitation of the wide-angle method is that the region of q values covered is limited by the wavelength (energy) of the radiation used so that when a conventional source of radiation is employed (e.g., x-ray tube with Mo anode) diffraction spectra to values of q not higher than $15\text{-}16 \text{ \AA}^{-1}$ are recorded. As a result, atomic distribution functions with reso-

lution δr , estimated by $\delta r = \pi/q_{\text{max}}$ not better than 0.19 Å could be obtained. That is why the individual Si-O and Al-O units, having characteristic distances $r_{\text{Si-O}} = 1.61 \pm 0.03$ Å, $r_{\text{Al-O}} = 1.75 \pm 0.03$ Å for tetrahedral coordination,¹⁷⁻¹⁹ could not possibly be differentiated by conventional x-ray diffraction studies^{15,16} carried out so far and, hence, the above discussed ambiguity has not been possible to be solved. A possible way to extend the high- q limit in diffraction studies and to improve the real space resolution of atomic distribution functions is to employ the so-called energy dispersive x-ray diffraction (EDXD) method. With the EDXD method the diffraction spectrum is recorded as a function of energy E of x-ray photons scattered at a fixed diffraction angle 2Θ . The sample is irradiated with x rays of continuous energy (wavelength) spectrum and an energy-sensitive detector is used to register the scattered x-ray photons of different energies. Among other advantages (reduced experimental time, simplified mechanical construction, etc.) the EDXD method has the important one that even when a conventional source of x-ray radiation is employed the structure factor can be obtained over a region of q values well extended above 20 \AA^{-1} and thus the resolution of the corresponding atomic distribution function be considerably improved.²⁰⁻²³ It is the purpose of the present work to obtain extended structure factors and atomic distribution functions of improved resolution for $\text{Ca}_{x/2}\text{Al}_x\text{Si}_{1-x}\text{O}_2$ glasses ($x=0, 0.34, 0.5, 0.68$) by carrying out EDXD experiments. It is expected that the employing of this experimental technique will make it possible for the type of the individual Si-O and Al-O units to be more precisely determined and, thus, for the model picture of the atomic scale structure of calcium aluminate-silicate glasses along the join $\text{SiO}_2\text{-CaAl}_2\text{O}_4$ to be clarified. This was quite a challenging task to tackle by the EDXD method.

II. EXPERIMENT

A. Samples preparation

$\text{Ca}_{x/2}\text{Al}_x\text{Si}_{1-x}\text{O}_2$ glasses ($x=0, 0.34, 0.5, 0.68$) were prepared by melting of appropriate precursors at 1900 K. The melts were rapidly cooled down to 1200 K and then the temperature was gradually reduced to 300 K at a rate of 0.5 K/min. The resulting glassy materials were with homogeneous macrostructure when looked at in visible light and, as the results of small-angle x-ray scattering experiments showed, no microinhomogeneities up to atomic scale were present. The glassy samples' actual chemical composition was checked by wet chemical analyses and found to differ from that one given above by less than 1%. The following data for the sample density, determined by the Archimedes method, have been obtained: $\rho(\text{SiO}_2; x=0) = 2.201 \text{ g/cm}^3$, $\rho(x=0.34) = 2.466 \text{ g/cm}^3$, $\rho(x=0.5) = 2.605 \text{ g/cm}^3$, and $\rho(x=0.68) = 2.711 \text{ g/cm}^3$. From the bulk glassy material produced thin plates, approximately 30 mm in length, 20 mm in width, and 1 mm in depth, were cut out and subjected to EDXD experiments.

B. EDXD data collection

The EDXD experiments were carried out in a laboratory setup consisted of a constant-potential generator (Siemens), a

sealed source of x rays with a copper anode, and a conventional automated goniometer device (Seifert FPM). The x-ray source was operated at 50 kV and 20 mA. A Ge solid-state detector (EG&G Ortec), firmly attached to one of the arms of the goniometer, was used to register the diffracted x-ray intensities. These were processed by a multichannel pulse-height analyzer (Ortec, Spectrum Master & Maestro Software) and stored in a computer readable format as a function of channel number. The registered intensities were transferred into energy space by using a channel number to energy calibration constant obtained by measuring the fluorescent lines of pure Fe, Ni, Zr, and Tb and fitting their channel numbers to the corresponding emission energies taken from literature sources. EDXD data of energies between 10 and 40 keV could be considered in the present studies since the Cu K_α line of the copper anode material was present at approximately 8 keV and the intensity of the x-ray photons of energies higher than 40 keV was too low. In order to keep the experimental resolution in reciprocal space as high as possible the experiments were carried out in a transmission geometry and a proper combination of slits was selected for each of the diffraction angles measured. Eight EDXD spectra, collected at fixed angles of $2\Theta = 6^\circ, 11^\circ, 20^\circ, 40^\circ, 60^\circ, 80^\circ, 100^\circ, \text{ and } 120^\circ$, were obtained for each of the glasses studied. The diffraction angles were so selected that any two consecutive regions of data in reciprocal (q) space, corresponding to two consecutive diffraction angles, well overlapped. Each spectrum was gathered over a period of time so long that at least 10 000 x-ray photons of energy 40 keV were stored in the corresponding channel of the detector system, having 1024 channels in our case. As a whole the total measuring time turned out to be of the order of 60 h per sample. As a corrective step, aimed at improving the statistical accuracy of the EDXD data without further increasing the experimental time, the x-ray intensities stored in each neighboring channel of the multichannel analyzer were averaged out taking advantage of the specific properties of the Savitzky and Golay moving average computational procedure.²⁴ The procedure was tuned in such a way that, on average, each data point gained or lost only one Poisson counting standard deviation in the averaging process. The physical grounds for applying of Savitzky and Golay averaging procedure is that the energy window of each channel of the multichannel analyzer (50 eV in our case) is much narrower than the actual energy resolution of the detector system (approximately 200 eV) so that x-ray photons of the same energy are, as a matter of fact, registered by few neighboring channels. That is why the photons stored in a few neighboring channels could be properly averaged out to produce data points of improved statistical accuracy. The applied averaging of the registered intensities and the relatively high intensity of the white x-ray spectrum delivered by the radiation source employed are that mainly contributed to the smooth behavior of the high- q part of the structure factors resulted from the present studies (see Fig. 2 later on introduced in the present paper).

C. EDXD data processing

All EDXD spectra measured are composed of x-ray photons coherently, incoherently, and multiply scattered from the particular sample and its environment. The relation be-

tween the EDXD intensities $I(E, \Theta)$ registered at a given (fixed) diffraction angle and their individual constituents can be expressed as follows:^{20–23}

$$I(E, \Theta) = c(E)\varepsilon(E)\{I(E)[I_{\text{coh}}(E, \Theta) + I_{\text{ms}}(E, \Theta) + I_{\text{bgr}}(E, \Theta)] + I(E')I_{\text{inc}}(E, E', \Theta)\}, \quad (2)$$

where $c(E)$ is a normalization factor, $\varepsilon(E)$ is the detector efficiency factor, $I(E)$ is the intensity of incident x rays of energy E , $I_{\text{coh}}(E, \Theta)$, $I_{\text{ms}}(E, \Theta)$, and $I_{\text{inc}}(E, E', \Theta)$ are the intensities of x-ray photons coherently, multiply, and incoherently scattered from the sample, and $I_{\text{bgr}}(E, \Theta)$ is the background intensity. Since the incoherent and multiple scattering from any sample with known physical characteristics (chemical composition, dimensions, density, etc.) can be calculated with good enough accuracy²³ and the background scattering can be experimentally measured, the only problem to be solved with the extraction of $I_{\text{coh}}(E, \Theta)$ from $I(E, \Theta)$ is the derivation of the unknown quantity $I_p(E) = c(E)\varepsilon(E)I(E)$, hereafter referred to as the spectrum of the incident radiation beam. Since the direct experimental determination of $I_p(E)$ is not an easy task the approach of determining the spectrum of the incident radiation beam from an experimental EDXD spectrum of the particular sample investigated has been adopted. This approach is based on the fact that the x-ray intensities (coherently, incoherently, multiply) scattered by the sample are only a small fraction of the total EDXD intensities registered at higher diffraction angles (say, $2\Theta > 60^\circ$), so that an EDXD spectrum measured at such angles will show only small modulations about $I_p(E)$.^{20–23} Within the frames of this approach Eq. (2) can be solved for the unknown quantity $I_p(E)$ in two equivalent forms:

$$I_p(E') = I_{\text{cor}}(E, \Theta) / \{I_{\text{inc}}(E, E', \Theta) + I_p(E)/I_p(E')\} \times [I_{\text{coh}}(E, \Theta) + I_{\text{ms}}(E, E', \Theta)], \quad (3a)$$

$$I_p(E) = I_{\text{cor}}(E, \Theta) / \{I_{\text{coh}}(E, \Theta) + I_p(E')/I_p(E)\} \times [I_{\text{inc}}(E, E', \Theta) + I_{\text{ms}}(E, E', \Theta)], \quad (3b)$$

where $I_{\text{cor}}(E, \Theta)$ are the EDXD intensities already appropriately corrected for background and for the escape-peak effect and the diffraction angle 2Θ has a high value.^{23,25} When the glassy material is composed of light atomic species and the incoherent scattering from the sample is stronger than the coherent one, as it is in the case with the glasses presently investigated, $I_p(E)$ can be calculated through an iterative procedure²⁵ based on Eq. (3b) with an initial assumption $I_p(E')/I_p(E) = 1$ and by substituting $I_{\text{coh}}(E, \Theta)$, $I_{\text{inc}}(E, E', \Theta)$, and $I_{\text{ms}}(E, E', \Theta)$ for their calculated values. When the amorphous material is composed of heavy atomic species Eq. (3a) is applied. As an example, the derivation of the structure factor for silica glass is described as follows. Multiplied by proper correction factors accounting for the absorption and polarization of x-ray radiation the calculated $I_{\text{inc}}(E, E', \Theta)$, $I_{\text{ms}}(E, E', \Theta)$, and $I_{\text{coh}}(E, \Theta)$, substituted for $I_{\text{coh}}(E, \Theta) = \sum_i c_i f_i^2(E, \Theta)$, where c_i and $f_i(E, \Theta)$ are the concentration and atomic scattering factor of atomic species i , as well as $I_{\text{cor}}(E, \Theta)$, the experimental EDXD spectrum for silica glass obtained at $2\Theta = 120^\circ$ and $I_p(E)$ was calculated. With the $I_p(E)$ data already determined the combined

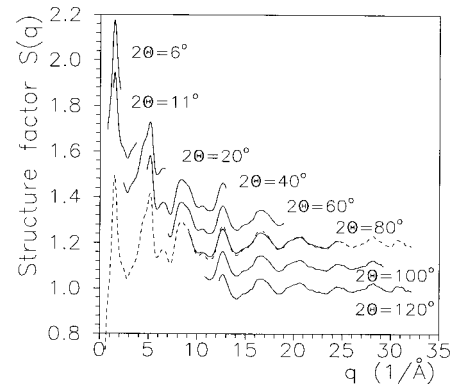


FIG. 1. Segments of the structure factor for silica glass determined from EDXD spectra obtained at eight different diffraction angles (full lines) and a total structure factor $S(q)$ obtained by their coupling (broken line). The segments corresponding to angles 2Θ other than 120° and the total $S(q)$ have been shifted up by a constant factor for clarity.

contribution of the incoherent and multiple scattering, i.e., $I_p(E)[I_{\text{coh}}(E, E', \Theta) + I_{\text{inc}}(E, E', \Theta)]$, has been calculated. By subtracting it from the experimental EDXD data the only coherently scattered intensities have been obtained. Then these have been reduced to the coherent single scattering per atom and a segment of the frequently used Faber-Ziman type²⁶ structure factor $S(q)$ has been calculated. With $I_p(E)$ determined from the EDXD data obtained at a diffraction angle 2Θ of 120° all the other seven EDXD spectra for silica glass have been similarly processed and corresponding segments of $S(q)$ have been obtained. All segments of $S(q)$ for silica glass thus obtained are shown in Fig. 1. The different segments of $S(q)$ have been coupled together, averaged out, and a total structure factor has been constructed. A comparison between the total $S(q)$ and one of its constituents (see Fig. 1) exemplifies the maximal discrepancy between the different $S(q)$ segments and their compound average observed with the present EDXD experiments. The part of $S(q)$ below the lowest q value covered by the present EDXD experiments, in the present case below $q = 0.76 \text{ \AA}^{-1}$, has been derived by a smooth extrapolation to $q = 0$. The resulting reduced structure factor for silica glass is shown in Fig. 2. The reduced structure factors for the other three glassy

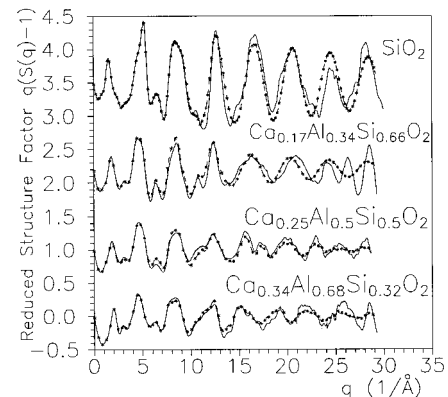


FIG. 2. Structure factors for $\text{Ca}_{x/2}\text{Al}_x\text{Si}_{1-x}\text{O}_2$ glasses ($x=0, 0.34, 0.5, 0.68$). Experimental EDXD data, full line and maximum entropy method processed data, broken line with symbols.

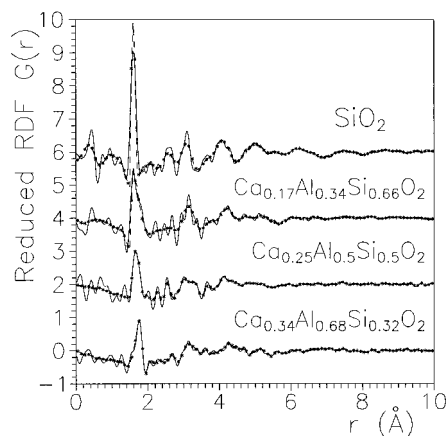


FIG. 3. Reduced atomic distribution function $G(r)$ for $\text{Ca}_{x/2}\text{Al}_x\text{Si}_{1-x}\text{O}_2$ glasses ($x=0,0.34,0.5,0.68$) obtained by Fourier transforming the experimental $S(q)$ data of Fig. 2 (full line) and by the maximum entropy method (broken line with symbols).

samples investigated, obtained in the same way as that of silica glass, i.e., by processing the eight corresponding EDXD spectra measured at the same diffraction angles 2θ , are also shown in Fig. 2. The corresponding reduced atomic distribution functions $G(r)$ are given in Fig. 3. It may be added that all calculations with the experimental EDXD data processing and derivation of the $S(q)$ data have been performed with the help of an improved version of the program PEDX.²³

III. RESULTS

As one can see from Fig. 2 the experimental reduced structure factors for $\text{Ca}_{x/2}\text{Al}_x\text{Si}_{1-x}\text{O}_2$ glasses ($x=0,0.34,0.5,0.68$) exhibit prominent oscillations up to the maximum q value of 30 \AA^{-1} reached. Before analyzing the experimental data in more detail we carefully checked their reliability as follows. First the present structure data for silica glass were compared with data obtained by an independent wide-angle x-ray diffraction study.²⁷ The comparison is shown in Fig. 4. As one can see from the figure the EDXD data and the previous wide-angle data are in good qualitative agreement which indicates that the present EDXD studies has yielded structure data that are at least so reliable as these ones ob-

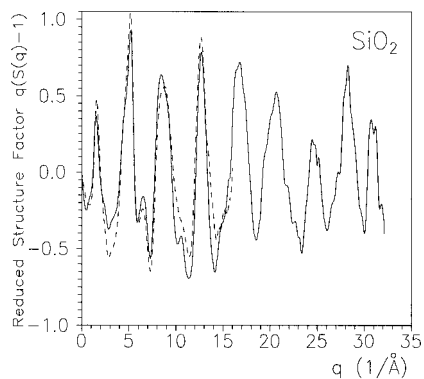


FIG. 4. Comparison between reduced structure factors $q[S(q)-1]$ for silica glass obtained by the present EDXD experiments (full line) and by previous wide-angle x-ray diffraction experiments (Ref. 27) (broken line).

tained by the conventional wide-angle x-ray diffraction method. With the EDXD method the region of reciprocal space covered is, however, much more extended than in the case of wide-angle experiments which, as one will see in the following discussions (see Figs. 5 and 6 introduced later in the text), has important implications on the real space resolution of the atomic distribution functions. By inspecting Fig. 4, however, one can notice that some quantitative differences between both sets of data are present. The observed discrepancy may be due to some differences in the respective data reduction procedures, to the fact that two different silica glass samples have been investigated by the present EDXD and the previous wide-angle experiments, and/or to the presence of some small residual statistical or systematic errors in both or one of the data sets. The last of these possibilities deserves special attention. It is well known that any systematic and statistical errors in $S(q)$ data, if present, propagate in the corresponding atomic distribution functions, and, together with the Fourier termination ripples, corrupt its fine features.²⁸ Since the present study addresses the fine structural features of $\text{Ca}_{x/2}\text{Al}_x\text{Si}_{1-x}\text{O}_2$ glasses ($x=0,0.34,0.5,0.68$) a more stringent check of the accuracy of the present EDXD data was mandatory. The check was carried out with the use of statistical procedures based on the maximum entropy method (MEM) which have proved to be quite efficient in identifying and removing statistical and systematic errors from structure data for disordered materials.²⁹⁻³¹ Structure factors and atomic distribution functions derived by subjecting the experimental ones to maximum-entropy-type analyses are shown in Figs. 2 and 3. The particular MEM calculations were carried out with the help of the newly developed program IFO.³¹ As one can see in Fig. 3 the application of MEM reduces the amplitudes of the spurious oscillations and termination ripples in real space which is well documented by the smooth behavior of the $G(r)$ data at low values of r . As one can see in Fig. 2 the original $S(q)$ data and the MEM processed $S(q)$ data are almost identical for values of q ranging from 0 to approximately 25 \AA^{-1} . This observation indicates that the residual systematic and statistical errors in the experimental $S(q)$ data, responsible for the small amplitude ripples in real space [see the low- r part of the original $G(r)$ functions], are concentrated presumably at values of q higher than 25 \AA^{-1} . There are several reasons for the possible presence of some errors in the experimental $S(q)$ data at high values of q . One is that the tabulated incoherent intensities, atomic scattering, and absorption factors for x rays may not be very accurate for values of q higher than 25 \AA^{-1} , i.e., for energies higher than 40–50 keV, since these standard data, as available at present,^{32,33} are derived on the basis of somewhat coarse extrapolation schemes. Some deficiencies in the EDXD data processing, in particular, the computational scheme for the derivation of the unknown intensity distribution of the primary x-ray beam may also be present. Summarizing, one may state that the EDXD studies carried out along the way described above (Sec. II) could guarantee good quality structure data extended to q values as high as 25 \AA^{-1} in case of glassy materials composed of light atomic species. An improvement in the EDXD data processing procedures and in the accuracy of the tabulated Compton intensities, atomic scattering, and absorption factors for x rays of energies higher than 40 keV is obviously to be done in order

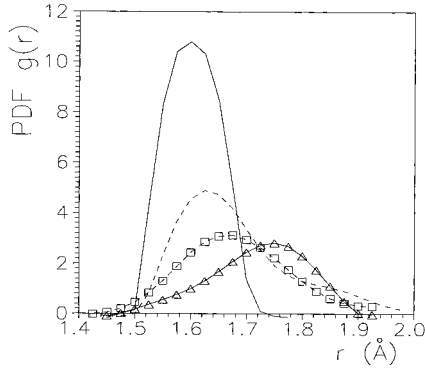


FIG. 5. First peaks in the pair distribution functions $g(r)$ for $\text{Ca}_{x/2}\text{Al}_x\text{Si}_{1-x}\text{O}_2$ glasses ($x=0,0.34,0.5,0.68$) obtained by Fourier transforming the experimental $S(q)$ data with $q_{\text{max}}=25 \text{ \AA}^{-1}$. Full line: $x=0$ (silica glass); broken line: $x=0.3$; full line with squares: $x=0.5$ (anorthite glass); full line with triangles: $x=0.68$.

that the attractive potential of EDXD method is fully explored. Taking into account the outcomes of the accuracy check carried out we decided to make use of $S(q)$ data of q values not higher than 25 \AA^{-1} only in order that the influence of the possible experimental and computational artifacts on the atomic distribution functions is reduced to a minimum. It may be added that $G(r)$'s obtained by a direct Fourier transformation of $S(q)$ data confined to $q_{\text{max}}=25 \text{ \AA}^{-1}$ and the MEM derived $G(r)$'s based on the full set of $S(q)$ data (shown in Fig. 3) turned out to be almost indistinguishable which corroborated the feasibility of our choice for the value of q_{max} . The overall quality of the atomic distribution functions thus obtained (MEM derived or $q_{\text{max}}=25 \text{ \AA}^{-1}$ based) was judged by calculating the average atomic number density ρ_0 on the basis of the expression

$$G(r) = -4\pi r \rho_0, \quad (4)$$

which holds only for small values of r .²⁸ The estimated values of ρ_0 for all glassy samples investigated deviated from the corresponding experimental ones by 4 to 6% at maximum. The so-called deviations could serve as an objective goodness-of-merit factor for the quality of the atomic distribution functions yielded by the present EDXD studies. Their small values give as enough confidence to state that the details of the experimental atomic distribution functions discussed below correspond to characteristic features of the respective glassy structures and are not experimental or computational artifacts. Here, one more point illustrating the advantages of the EDXD method deserves to be mentioned. In Fig. 5 the first peaks in the pair distribution functions $g(r)=\rho(r)/\rho_0$, obtained as specified above, are given. In Fig. 6, the same peaks, obtained by Fourier transforming a reduced part of the experimental $S(q)$'s, extended to $q_{\text{max}}=16 \text{ \AA}^{-1}$ only, are also given. As one can see in the figures the first peaks in the $g(r)$'s obtained on the basis of $S(q)$ data extended to $q_{\text{max}}=25 \text{ \AA}^{-1}$ show a clear asymmetry which indicates that two different structural units are present in the glasses investigated, something which has already been suggested by previous studies.¹⁻⁷ The first peaks in the $g(r)$'s obtained on the basis $S(q)$ data, extended to $q_{\text{max}}=16 \text{ \AA}^{-1}$ only, which is the usual high- q limit approached by the laboratory wide-angle experiments, do not show any

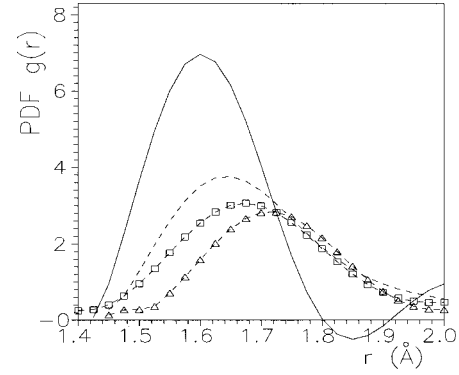


FIG. 6. First peaks in the pair distribution functions $g(r)$ for $\text{Ca}_{x/2}\text{Al}_x\text{Si}_{1-x}\text{O}_2$ glasses ($x=0,0.34,0.5,0.68$) obtained by Fourier transforming the experimental $S(q)$ data with $q_{\text{max}}=16 \text{ \AA}^{-1}$. Full line: $x=0$ (silica glass); broken line: $x=0.3$; full line with squares: $x=0.5$ (anorthite glass); full line with triangles: $x=0.68$.

signatures of asymmetry and appeared with reduced height and an increased full width at half maximum (about 25%) when compared to the corresponding ones of Fig. 5. The comparison well demonstrates the potential of the EDXD method in obtaining atomic distribution functions with considerably improved resolution.

IV. DISCUSSION

By inspecting Fig. 2 one can notice that systematic changes in the structure factors of $\text{Ca}_{x/2}\text{Al}_x\text{Si}_{1-x}\text{O}_2$ glasses ($x=0,0.34,0.5,0.68$) take place with the change of Ca and Al content. The first sharp diffraction peak positioned at 1.55 \AA^{-1} with silica glass shifts to 1.77 \AA^{-1} with $\text{Ca}_{0.17}\text{Al}_{0.34}\text{Si}_{0.66}\text{O}_2$ glass, then to 1.85 \AA^{-1} with anorthite glass, and finally 2.0 \AA^{-1} with $\text{Ca}_{0.34}\text{Al}_{0.68}\text{Si}_{0.32}\text{O}_2$ glass. The amplitude of this peak gradually reduces with increasing Ca and Al content. The same systematic changes have been observed with the previously carried out wide-angle x-ray diffraction experiments.¹⁶ The peak in the structure factor for silica glass at 5.17 \AA^{-1} , which is the strongest among the others, reduces in height with the increase of Al and Ca content and its position slightly shifts towards lower q values. The subsequent strong peak positioned at approximately 8.4 \AA^{-1} also diminishes with the increase of Ca and Al content but its position remains almost unchanged. The well defined peaks at $12.7, 16.35, 20.6,$ and 24.6 \AA^{-1} in the structure factor of silica glass are seen with substantially reduced amplitudes, smeared shapes, and shifted positions with $\text{Ca}_{x/2}\text{Al}_x\text{Si}_{1-x}\text{O}_2$ glasses ($x=0.34,0.5,0.68$). The shift in the peak position is so substantial that the structure factors for silica glass and $\text{Ca}_{0.34}\text{Al}_{0.68}\text{Si}_{0.32}\text{O}_2$ glass oscillate almost out-of-phase at q values higher than 15 \AA^{-1} . It is well known that the oscillation in $S(q)$ at higher q values are presumably determined by the shortest interatomic distances in the particular glassy system. The fact that $S(q)$ for silica glass and $\text{Ca}_{0.34}\text{Al}_{0.68}\text{Si}_{0.32}\text{O}_2$ glass are out-of-phase in the higher q region unambiguously indicates that interatomic distances substantially different from Si-O ones are that determine the oscillation behavior of $S(q)$ for $\text{Ca}_{0.34}\text{Al}_{0.68}\text{Si}_{0.32}\text{O}_2$ glass at higher q values. This indication is corroborated by an inspection of the shape of the first peak in the experimental pair

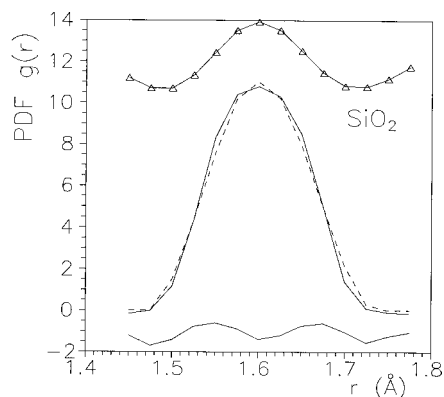


FIG. 7. Gaussian fit to the first peak in the PDF $g(r)$ for silica glass. Experimental data: full line; fitted data: broken line; residual difference: full line (bottom). The local fourth derivative of the experimental data is also given in the upper part (full line with symbols).

distribution functions $g(r)$ presented in Figs. 5, 7–10. As one can see in the figures the first peaks in the $g(r)$'s for $\text{Ca}_{x/2}\text{Al}_x\text{Si}_{1-x}\text{O}_2$ glasses ($x=0.34, 0.5, 0.68$) exhibit a clear asymmetry indicating that these peaks are composed of two components. As one can see well in Fig. 5 the first of these components, peaking at approximately 1.6 Å, becomes lower in intensity while the intensity of the second one, peaking at approximately 1.75 Å, increases with the increase of Ca and Al content. By referring to the first peak in $g(r)$ for silica glass and to results of previous studies^{6,7,15–19} one may attribute the low- r component of the first peak in $g(r)$ for $\text{Ca}_{x/2}\text{Al}_x\text{Si}_{1-x}\text{O}_2$ glasses ($x=0.34, 0.5, 0.68$) to the first neighbor Si-O atomic correlations. The component at higher r values then may be attributed to the first neighbor Al-O atomic correlations. Thus the present EDXD experiments have yielded atomic distribution functions with resolutions good enough for the two distinct Si-O and Al-O structural units in the glasses investigated to be differentiated. The main characteristic of these structural units, namely, the oxygen coordination number, has been determined by fitting the corresponding components of the first peaks in the experimental $g(r)$ functions with analytical functions of Gaussian type. The results of the fitting are presented in Figs. 7–10. The

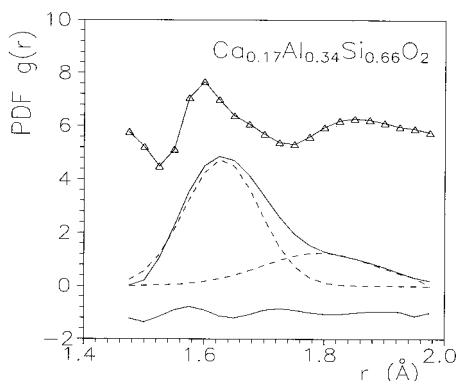


FIG. 8. Gaussian fit to the first peak in the PDF $g(r)$ for $\text{Ca}_{0.17}\text{Al}_{0.34}\text{Si}_{0.66}\text{O}_2$ glass. Experimental data: full line; fitted data: broken line; residual difference: full line (bottom). The local fourth derivative of the experimental data is also given in the upper part (full line with symbols).

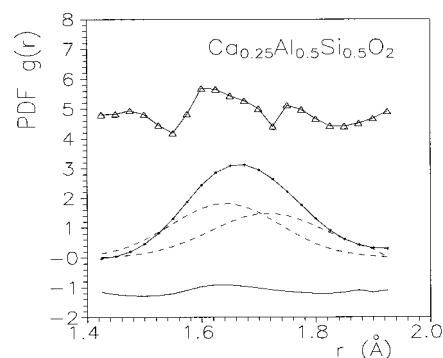


FIG. 9. Gaussian fit to the first peak in the PDF $g(r)$ for anorthite glass. Experimental data: full line; fitted data: broken line; residual difference: full line (bottom). The local fourth derivative of the experimental data is also given in the upper part (full line with symbols).

goodness-of-fit indicator achieved is of the order of 5% for all fits carried out. In the case of the glasses containing Ca and Al the positions of the maxima of the local fourth derivative of the experimental data, which are very sensitive to the change in the shape of compound peaks, indicated the initial positions of the two Gaussians. These initial positions were further refined in the course of the fitting process. To make the outcomes of the fitting process more unambiguous, the Gaussians approximating the Si-O first neighbor atomic correlations have been forced to spread over a real space region extended from approximately 1.5 to 1.8 Å only where Si-O first neighbor atomic correlations are found to be present in silicate glasses.² It may be mentioned, however, that this constraint on the fitting process turned out to have a minor effect on the results obtained. The first neighbor Si-O and Al-O interatomic distances and coordination numbers resulted from the fits are presented in Table I. Concerning the results for the first neighbor Si-O interatomic distance ($r_{\text{Si-O}}=1.601\pm 0.005$ Å) and coordination number ($Z_{\text{Si-O}}=4.02\pm 0.1$) in silica glass obtained from the present EDXD data a fairly good agreement with those ($r_{\text{Si-O}}=1.607\pm 0.005$ Å, $Z_{\text{Si-O}}=3.87\pm 0.2$) obtained by highly accurate time-of-flight neutron diffraction experiments³⁴ is to be noted. This agreement is strong evidence in support of the

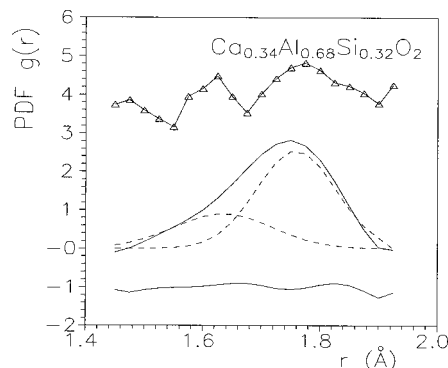


FIG. 10. Gaussian fit to the first peak in the PDF $g(r)$ for $\text{Ca}_{0.34}\text{Al}_{0.68}\text{Si}_{0.32}\text{O}_2$ glass. Experimental data: full line; fitted data: broken line; residual difference: full line (bottom). The local fourth derivative of the experimental data is also given in the upper part (full line with symbols).

TABLE I. First neighbor Si-O and Al-O interatomic distances r (in Å) and coordination numbers Z in $\text{Ca}_{x/2}\text{Al}_x\text{Si}_{1-x}\text{O}_2$ glasses ($x=0,0.34,0.5,0.68$) obtained by a Gaussian fit to the first peaks in the corresponding experimental pair distribution functions $g(r)$.

	$r_{\text{Al-O}}$	$Z_{\text{Al-O}}$	$r_{\text{Si-O}}$	$Z_{\text{Si-O}}$
SiO_2			1.601 ± 0.005	4.02 ± 0.1
$\text{Ca}_{0.17}\text{Al}_{0.34}\text{Si}_{0.66}\text{O}_2$	1.773 ± 0.005	4.05 ± 0.1	1.632 ± 0.005	3.92 ± 0.1
$\text{Ca}_{0.25}\text{Al}_{0.5}\text{Si}_{0.5}\text{O}_2$	1.722 ± 0.005	3.90 ± 0.1	1.647 ± 0.005	3.90 ± 0.1
$\text{Ca}_{0.34}\text{Al}_{0.68}\text{Si}_{0.32}\text{O}_2$	1.762 ± 0.005	3.90 ± 0.1	1.630 ± 0.005	2.82 ± 0.1

reliability of the present EDXD experiments. The results presented in Table I offer an opportunity to trace the evolution of the Si-O and Al-O structural units with the change in the composition of the glasses investigated. As these results show when the concentration of Al and Ca atoms is relatively low ($\text{Ca}_{0.17}\text{Al}_{0.34}\text{Si}_{0.66}\text{O}_2$ glass) both Si and Al atoms are with fourfold oxygen coordination. Fourfold oxygen coordination of Si and Al atoms is found with anorthite glass ($\text{Ca}_{0.25}\text{Al}_{0.5}\text{Si}_{0.5}\text{O}_2$) as well. Therefore, according to the results of the present study, one can view glasses with chemical compositions ranging from that of SiO_2 to that of anorthite as an assembly of well-defined SiO_4 and AlO_4 units which is well in line with the structure models that have been previously proposed.^{1,6,7,9,15,16} When $(\text{CaO} + \text{Al}_2\text{O}_3)$ content exceeds that of SiO_2 ($\text{Ca}_{0.34}\text{Al}_{0.68}\text{Si}_{0.32}\text{O}_2$ glass) Al atoms are again fourfold coordinated while the number of oxygen atoms around Si atoms is considerably reduced from the typical value of 4. This result of the present study correlates well with the findings of previous ^{29}Si NMR and ESR experiments^{6,12} pointing the presence of nonbridging oxygen in the first coordination shell of Si atoms in glasses with high Ca and Al content. Summarizing one may conclude that Al atoms always have fourfold oxygen coordination while the oxygen coordination of Si atoms changes, from fourfold to considerably lower, in the glasses along the join SiO_2 - CaAl_2O_4 . Taking into account this main outcome of the present studies one can easily explain the shift in the oscillating behavior of the experimental structure factors at high q values. At the SiO_2 end of the join SiO_2 - CaAl_2O_4 well defined SiO_4 structural units are the main building units of the glassy structure and the shortest Si-O separation within the SiO_4 units is what determines the oscillation behavior of the structure factor $S(q)$ at higher values of q . At the Al_2O_3 end of the join SiO_2 - CaAl_2O_4 the Si-O units are highly defect and the well-defined AlO_4 units turn out to be the main building units of the glassy structure. Correspondingly, the shortest Al-O separation within AlO_4 units determines the oscillating behavior of the structure factor $S(q)$ at high q values. At intermediate concentrations of Ca and Al (close to anorthite glass) the high- q behavior of $S(q)$ is an interference pattern

resulted from the shortest Si-O and Al-O separations within the SiO_4 and AlO_4 units present. Another interesting outcome of the present study is the fact that the Si-O separation with anorthite glass turns out to be the longest among the Si-O ones found with all glasses presently investigated. On the other hand, the Al-O separation with anorthite glass turns out to be the shortest among the Al-O separations found with all glasses investigated. This observation suggests that some specific chemical short-range order effects are quite probably present in the anorthite glass. Results from thermodynamic investigations on $\text{CaO-Al}_2\text{O}_3\text{-SiO}_2$ glasses with a composition close to that of anorthite have given a very similar interpretation.¹

V. CONCLUSION

Good quality structure factors extended up to 25 \AA^{-1} have been obtained for glasses composed of light atomic species by energy-dispersive x-ray diffraction experiments. The improved resolution in real space has made it possible for the type of Si-O and Al-O units in $\text{Ca}_{x/2}\text{Al}_x\text{Si}_{1-x}\text{O}_2$ glasses ($x = 0.34, 0.5, 0.68$) to be unambiguously determined. It has been found that glasses with composition varying from that of SiO_2 to that of anorthite ($\text{Ca}_{0.25}\text{Al}_{0.5}\text{Si}_{0.5}\text{O}_2$) are constituted of defectless SiO_4 and AlO_4 units. Glasses where $(\text{CaO} + \text{Al}_2\text{O}_3)$ exceeds the SiO_2 content are formed of defectless AlO_4 polyhedra and Si-O units with a considerable number of nonbridging oxygens. Thus the results of the present study do not corroborate the model picture viewing the glasses along the join SiO_2 - CaAl_2O_4 as a fully polymerized network of tetrahedral SiO_4 and AlO_4 units. A model picture viewing the glasses along the join SiO_2 - CaAl_2O_4 as an assembly AlO_4 tetrahedra and Si-O units of variable oxygen coordination is given definitive support.

ACKNOWLEDGMENTS

The financial support of the Alexander von Humboldt Stiftung to one of the authors (V.P.) is gratefully acknowledged.

¹A. Navrotsky, G. Peraudeau, P. McMillan, and J.-P. Coutures, *Geochim. Cosmochim. Acta* **46**, 2039 (1982).

²B. O. Mysen, *Structure and Properties of Silicate Melts* (Elsevier, Amsterdam, 1988).

³C. Huang and E. C. Behrman, *J. Non-Cryst. Solids* **128**, 310 (1991).

⁴M. E. Lines, *J. Non-Cryst. Solids* **103**, 279 (1988).

⁵M. E. Lines, J. B. McChesney, K. B. Lyons, A. J. Bruce, A. E. Miller, and K. Nassau, *J. Non-Cryst. Solids* **107**, 251 (1989).

⁶G. Engelhardt, M. Nofz, K. Forkel, F. G. Wihsmann, M. Mägi, A. Samoson, and E. Lippmaa, *Phys. Chem. Glasses* **26**, 157 (1985).

- ⁷M. Nofz, K. Forkel, E. G. Wihsmann, and H.-G. Bartel, *Phys. Chem. Glasses* **30**, 46 (1989).
- ⁸C. I. Merzbacher, B. L. Sherriff, J. S. Hartman, and W. B. White, *J. Non-Cryst. Solids* **124**, 194 (1990).
- ⁹P. McMillan, B. Piriou, and A. Navrotsky, *Geochim. Cosmochim. Acta* **46**, 2021 (1982).
- ¹⁰F. Seifert, B. O. Mysen, and D. Virgo, *Am. Mineral.* **67**, 696 (1982).
- ¹¹G. W. Tasker, D. R. Uhlmann, P. I. K. Onorato, M. N. Alexander, and C. W. Struck, *J. Phys. C* **8**, 273 (1985).
- ¹²M. Nofz, R. Stösser, and F. G. Wihsmann, *Phys. Chem. Glasses* **31**, 57 (1990).
- ¹³B. Velde and R. Couty, *Chem. Geol.* **62**, 35 (1987).
- ¹⁴H. Morikawa, S.-I. Miwa, M. Miyake, F. Marumoto, and T. Sata, *J. Am. Ceram. Soc.* **65**, 78 (1982).
- ¹⁵M. Taylor and G. E. Brown, Jr., *Geochim. Cosmochim. Acta* **43**, 61 (1979); **43**, 1467 (1979); **44**, 109 (1980).
- ¹⁶B. Himmel, J. Weigelt, Th. Gerber, and M. Nofz, *J. Non-Cryst. Solids* **136**, 27 (1991).
- ¹⁷C. J. E. Kempster, H. D. Megaw, and E. W. Radoslovich, *Acta Crystallogr.* **15**, 1005 (1962).
- ¹⁸J. D. Megaw, C. J. E. Kempster, and E. W. Radoslovich, *Acta Crystallogr.* **15**, 1017 (1962).
- ¹⁹R. Wyckoff, *Crystal Structures* (Wiley, New York, 1954).
- ²⁰T. Egami, *J. Mater. Sci.* **13**, 2587 (1978).
- ²¹R. Utz, A. Brunsch, P. Lamparter, and S. Steeb, *Z. Naturforsch., A: Phys. Sci.* **44**, 1201 (1989).
- ²²V. Petkov, *J. Non-Cryst. Solids* **192&193**, 65 (1995).
- ²³V. Petkov and Y. Waseda, *J. Appl. Crystallogr.* **26**, 295 (1993).
- ²⁴A. Savitzky and M. Golay, *Anal. Chem.* **36**, 1627 (1964).
- ²⁵C. N. J. Wagner, D. Lee, S. Tai, and L. Keller, *Adv. X-Ray Anal.* **24**, 245 (1981).
- ²⁶Y. Waseda, *The Structure of Non-Crystalline Materials* (McGraw-Hill, New York, 1980).
- ²⁷J. Konnert and J. Karle, *Acta Crystallogr., Sect. A: Cryst. Phys., Diffr., Theor. Gen. Crystallogr.* **29**, 702 (1973).
- ²⁸H. Klug and L. Alexander, *X-ray Diffraction Procedures for Polycrystalline and Amorphous Materials* (Wiley, New York, 1974).
- ²⁹W. Wei, *J. Non-Cryst. Solids* **81**, 239 (1986).
- ³⁰J. Jal, A. Soper, P. Carmona, and J. Dupuy, *J. Phys.: Condens. Matter* **3**, 551 (1991).
- ³¹V. Petkov and R. Danev, *J. Appl. Crystallogr.* **31**, 609 (1998).
- ³²D. Cromer and J. B. Mann, *Acta Crystallogr., Sect. A: Cryst. Phys., Diffr., Theor. Gen. Crystallogr.* **24**, 321 (1968).
- ³³*International Tables for Crystallography* (Kluwer Academic, Dordrecht, 1992), Vol. C.
- ³⁴D. Grimley, A. Wright, and R. Sinclair, *J. Non-Cryst. Solids* **50**, 281 (1982).